Journal of Nuclear Materials 390–391 (2009) 364–367

Contents lists available at ScienceDirect

Journal of Nuclear Materials

journal homepage: www.elsevier.com/locate/jnucmat

Statistical analysis to the SOL plasma fluctuation in JT-60U

N. Asakura [a,*], N. Ohno [b], H. Tanaka [b], H. Kawashima [a], T. Nakano [a]

[a] Japan Atomic Energy Agency, Mukouyama 801-1, Naka, Ibaraki-ken 311-0193, Japan
[b] Graduate School of Engineering, Nagoya Univ., Nagoya 464-8603, Japan

ARTICLE INFO

PACS:
52.25.−b

ABSTRACT

Intermittent events and their temporal scale were studied in the L-mode SOL plasma by applying statistical analysis of probability distribution function and conditional average to j_s and V_f measured with the Mach probes at the HFS and LFS. Fluctuation level was large (20–70%) at the LFS midplane, compared to those near the *X*-point (4–20%) and the HFS SOL (4–10%). 'Burst events' were measured mostly at the LFS midplane, where positive *skewness* ($S = 0.3$–0.8) extended from the separatrix to the far SOL ($r^{mid} < 10$ cm). Time scale of the 'burst events' was short (~5 μs). When the divertor plasma was detached up to the vicinity of the X-point, large 'burst events' characterized by $S \sim 1.8$ and long time scale of 40–80 μs occurred in the outer SOL near the *X*-point ($0.5 < r^{mid} < 1.5$ cm). The large 'burst events' can therefore be considered as a candidate mechanism to enhance the radial transport and SOL flow in the divertor.

1. Introduction

Non-diffusive intermittent transport has been observed in the edge plasmas of many tokamaks [1,2], enhancing cross-field transport of heat and particle fluxes towards the first wall. Determination of its characteristics and of its poloidal distribution is of great importance for understanding the radial and perpendicular transport of the SOL plasma.

In JT-60U, statistical analysis of a probability distribution function (PDF) and conditional average was applied to determine intermittent events in fluctuations of ion saturation current (j_s) and floating potential (V_f) measured in the low-field-side (LFS) and high-field-side (HFS) SOLs [3]. Skewness and flatness are defined by the 3rd and 4th moments of the PDF, normalized by the standard deviation, i.e. $S = \langle x^3\rangle/\langle x^2\rangle^{3/2}$ and $F = \langle x^4\rangle/\langle x^2\rangle^2$, respectively. When large positive bursts occur in the fluctuation signal, the PDF is positively skewed and becomes flat compared to Gaussian distribution which is characterized by $S = 0$ and $F = 3$. On the other hand, conditional average shows the time scale of the large intermittent events and cross-correlation with events in the different signals.

In-out asymmetry in the radial transport of the edge and SOL plasmas can be responsible for observed asymmetry of heat and particle fluxes between the inner and outer divertors, as well as the parallel SOL flow [4]. In this paper, characteristics of the fluctuations at the HFS and LFS SOLs are investigated in L-mode plasmas. Fluctuation levels of the LFS and HFS SOL plasmas and the PDF results are presented in Section 2. Conditional average results are shown in Section 3. Changes in the fluctuation characteristics during the divertor detachment, in particular near the *X*-point, are described in Section 4. Results are summarized in Section 5.

2. Poloidal asymmetry in fluctuation characteristics

Characteristics of the fluctuations were measured with three Mach probes installed at LFS midplane, *X*-point and above HFS baffle [3] in L-mode plasmas: $I_p = 1$ MA, $B_t = 3.2$ T, $P_{NB} = 4$ MW, plasma triangularity (δ) of 0.32, elongation (κ) of 1.4, safety factor at 0.95 (q_{95}) of 4.7, and line-averaged density ($\bar{n}_e$) was varied in 1.2–2.4×10^{19} m^{-3} on a shot by shot basis. Reciprocation time of the Mach probe was 1 s and the sampling rate was 500 kHz.

Fig. 1 shows radial profiles of time-averaged j_s ($\langle j_s\rangle$) and its fluctuation level ($\delta j_s/\langle j_s\rangle$) over 2 ms (1000 data points), the radial coordinate being mapped to the radius at the LFS midplane (r^{mid}) for $\bar{n}_e = 1.7 \times 10^{19}$ m^{-3} (the Greenwald density fraction, $\bar{n}_e/n^{GW}$, of 0.40). Since the midplane Mach probe is located at 34 cm below the plasma midplane, $\langle j_s\rangle$ at the 'midplane-side' and 'divertor-side' ($\langle j_s^{mid\text{-}m}\rangle$ and $\langle j_s^{mid\text{-}d}\rangle$) are measured by probes facing the midplane and the outer divertor along the field lines, respectively. Values of $\langle j_s\rangle$ measured at the main-plasma-side of the *X*-point probe ($\langle j_s^{Xp\text{-}m}\rangle$) and at the midplane-side of the HFS Mach probe ($\langle j_s^{HFS\text{-}m}\rangle$) are also shown, and they are larger than those measured at the divertor-side ($\langle j_s^{Xp\text{-}d}\rangle$ and $\langle j_s^{HFS\text{-}d}\rangle$). Near the separatrix ($r^{mid} \leqslant 3$ cm), $\langle j_s\rangle$ profiles (except for $\langle j_s^{mid\text{-}d}\rangle$) are comparable and all profiles have relatively similar e-folding lengths of $\lambda_{js} = 2.0$–2.5 cm. On the other hand, poloidal asymmetry in $\delta j_s/\langle j_s\rangle$ is clearly observed: $\delta j_s/\langle j_s\rangle$ is enhanced particularly at the LFS midplane (40–70% for the midplane-side, and 20–40% for the divertor-side of the Mach probe).

* Corresponding author. Fax: +81 29 270 7419.
E-mail address: asakura.nobuyuki@jaea.go.jp (N. Asakura).

0022-3115/$ - see front matter © 2009 Elsevier B.V. All rights reserved.
doi:10.1016/j.jnucmat.2009.01.073

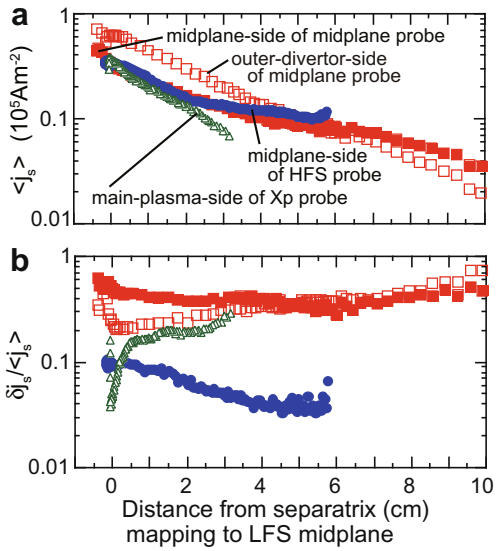

Fig. 1. Profiles of (a) averaged values of j_s ($\langle j_s \rangle$) over 2 ms (1000 data points) intervals at the midplane (closed squares) and outer-divertor (open squares) sides of the midplane Mach probe, at the main-plasma side of the *X*-point Mach probe (triangles), at the midplane-side of the HFS Mach probe (circles). (b) corresponding fluctuation levels ($\delta j_s/\langle j_s \rangle$). Radial coordinate is mapped to the radius at the LFS midplane for $\bar{n}_e = 1.7 \times 10^{19}$ m^{-3}.

Near the *X*-point, $\delta j_s/\langle j_s \rangle$ increases from 4% to 20% when moving away from the *X*-point. In the HFS SOL, $\delta j_s/\langle j_s \rangle$ is small (4–10%) and decreases when moving away from the separatrix.

Fig. 2 shows examples of PDFs at the tree poloidal locations, i.e. the LFS midplane, the *X*-point and the HFS SOL ($j_s^{mid\text{-}m}$, $j_s^{Xp\text{-}m}$ and $j_s^{HFS\text{-}m}$), at the same distance from the separatrix of 2 cm, corresponding to r^{mid} = 2.0, 0.2, 0.6 cm, respectively. The sample number is 5000. The fluctuation level is large at the LFS midplane ($\delta j_s^{mid\text{-}m}/\langle j_s^{mid\text{-}m} \rangle = 0.4$), compared to those near the *X*-point ($\delta j_s^{Xp\text{-}m}/\langle j_s^{Xp\text{-}m} \rangle = 0.1$) and at the HFS SOL ($\delta j_s^{HFS\text{-}m}/\langle j_s^{HFS\text{-}m} \rangle = 0.09$). A large deformation of the PDF from a Gaussian distribution is observed in $(j_s^{mid\text{-}m} - \langle j_s^{mid\text{-}m} \rangle)/\sigma_{js} < -2$ and $(j_s^{mid\text{-}m} - \langle j_s^{mid\text{-}m} \rangle)/\sigma_{js} \geqslant 2.5$ only at the LFS midplane, and positive *S* (=0.4) and larger *F* (=3.7) are found. A similar deformation of PDF was observed in $j_s^{mid\text{-}d}$. On the other hand, PDFs near the *X*-point and at the HFS SOL are similar to the Gaussian distribution.

Radial profiles of *S* for the three SOL locations are shown in Fig. 3. At the LFS midplane, positive *S* (=0.3–0.8) extends from

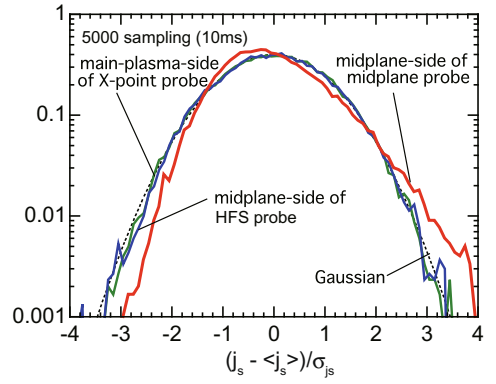

Fig. 2. Representative normalized PDFs of j_s at the midplane-side of the midplane Mach probe, the main-plasma side of the *X*-point Mach probe, and the midplane-side of the HFS Mach probe, for the same distance from the separatrix (2 cm), corresponding r^{mid} = 2.0, 0.2, 0.6 cm, respectively. Here, sampling data is 5000 (during 10 ms). Gaussian distribution function is shown by dotted line.

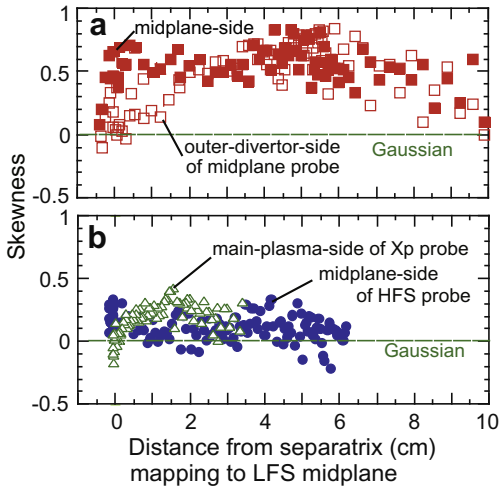

Fig. 3. Profiles of skewness (a) for the midplane (closed squares) and outer-divertor (open squares) sides of the midplane Mach probe, (b) for the main-plasma side of the *X*-point Mach probe (triangles) and at the midplane-side of the HFS Mach probe (circles). Those correspond to profiles in Fig. 1.

the separatrix to the far SOL (r^{mid} < 10 cm), whereas *S* at the outer-divertor-side is small in the vicinity of the separatrix (r^{mid} < 2 cm). Profiles of *S* for the *X*-point and the HFS SOL are calculated from $j_s^{Xp\text{-}m}$ and $j_s^{HFS\text{-}m}$, and they are small (*S* < 0.4) due to small deformation of PDF from the Gaussian distribution. As a result, large 'burst events' occur frequently in the vicinity of the separatrix at the LFS midplane, extending to the far SOL, but do not extend to the *X*-point and the HFS SOL.

3. Temporal characteristics of intermittent events

Temporal characteristics of 'burst events' at the LFS midplane are investigated by the conditional average, which is applied to j_s and V_f fluctuations. Here, a floating probe is located at the top of 5 mm ridge separating the midplane and outer-divertor-sides of the Mach probe. In this analysis, large positive burst events, i.e. $(j_s^{mid\text{-}m} - \langle j_s^{mid\text{-}m} \rangle) \geqslant 2.5\sigma_{js}$, are collected as the primary reference, and the first timing for satisfying the criterion is defined as $\tau = 0$, then time evolutions of the burst events are averaged. During the large burst events of $j_s^{mid\text{-}m}$, $j_s^{mid\text{-}d} - \langle j_s^{mid\text{-}d} \rangle$ and $V_f^{mid} - \langle V_f^{mid} \rangle$ are averaged to determine correlation with the $j_s^{mid\text{-}m}$ bursts.

Fig. 4 shows examples of normalized conditional average of $j_s^{mid\text{-}m}$, $j_s^{mid\text{-}d}$ and V_f^{mid} at $r^{mid} \sim 2$ cm during 20 ms, where 78 events are averaged. $\langle j_s^{mid\text{-}m} \rangle$, $\langle j_s^{mid\text{-}d} \rangle$ and $\langle V_f^{mid} \rangle = 32$ kA m^{-2}, 61 kA m^{-2} and 1.5 V, and $\sigma_{js\text{-}m}$, $\sigma_{js\text{-}d}$, and $\sigma_{Vf} = 15$ kA m^{-2}, 14 kA m^{-2} and

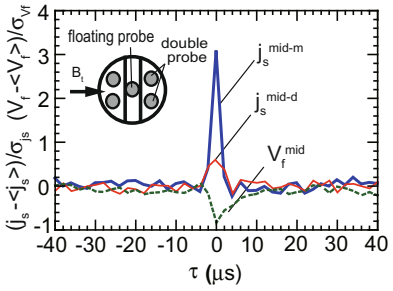

Fig. 4. Conditional average of j_s at the midplane-side of the midplane Mach probe, over 78 large positive burst events, i.e. $(j_s^{mid\text{-}m} - \langle j_s^{mid\text{-}m} \rangle) > 2.5\sigma_{js}$. j_s at the outer-divertor-side and V_f at the top are averaged. Here r^{mid} = 2.0 cm. Probe arrangement of the Mach probe is also shown.

10 V, respectively. The time scale of large positive events is found to be relatively short (~5 μs). Positive correlation between $j_s^{mid\text{-}m}$ and $j_s^{mid\text{-}d}$ is observed, while V_f^{mid} exhibits a negative burst of 10–20 V amplitude, suggesting that a plasma filament with temperature higher than the background one is passing the probe. It was also observed that the positive correlations between $j_s^{mid\text{-}m}$ and $j_s^{mid\text{-}d}$ and between $j_s^{mid\text{-}m}$ and negative V_f^{mid} are large near the separatrix ($r^{mid} < 2$ cm) and decrease with r^{mid}.

As a result, the large burst events would be explained by the plasma filaments passing the Mach probe in the radial and/or poloidal directions. Assuming the radial movement of the filament with the velocity of 1 km/s, the size of the burst cell is ~0.5 cm.

4. Fluctuation characteristics during divertor detachment

Fig. 5 shows radial profiles of $\langle j_s^{mid}\rangle$, $\delta j_s^{mid}/\langle j_s^{mid}\rangle$ and S for the two sides of the midplane Mach probe for $\bar{n}_e = 2.4\times10^{19}$ m^{-3} ($\bar{n}_e/n^{GW} = 0.54$), when partial detachment of the divertor plasma occurs near the separatrix. $\langle j_s^{mid}\rangle$ is increased over the whole radial profile and the difference of $\langle j_s^{mid}\rangle$ for the two sides becomes smaller compared to those for the lower $\bar{n}_e$ case shown in Figs. 1 and 2. Whereas $\delta j_s^{mid}/\langle j_s^{mid}\rangle$ of 20–40% for the two sides (in $r^{mid} < 10$ cm) is comparable to those for the lower $\bar{n}_e$, profiles of S change: positive S values at both the midplane- and outer-divertor-sides are increased from 0–0.7 (near the separatrix) to 0.4–1.2 at $r^{mid} = 9$ cm, extending towards the far SOL.

Radial profiles of $\langle j_s^{Xp\text{-}m}\rangle$, $\delta j_s^{Xp\text{-}m}/\langle j_s^{Xp\text{-}m}\rangle$, S^{Xp-m} and the Mach number of the parallel plasma flow ($M_{//}^{Xp}$) change significantly, as shown in Fig. 6, when the detachment occurs at the outer divertor and extends to near the X-point. Fig. 6(a) shows that $j_s^{Xp\text{-}m}$ near the X-point ($r^{mid} < 0.5$ cm) is reduced compared to that in the attached region ($r^{mid} > 0.6$ cm), and the local plasma pressure becomes lower by the factor of 2 compared to that at the LFS midplane. Fig. 6(b) and (c) shows that $\delta j_s^{Xp\text{-}m}/\langle j_s^{Xp\text{-}m}\rangle$ and $M_{//}^{Xp}$ exceed those in lower $\bar{n}_e$ plasmas. Large enhancements of S^{Xp-m} (up to 1.8) and $M_{//}^{Xp}$ (comparable to the sonic level) are observed in $0.5 < r^{mid} < 1.5$ cm, where

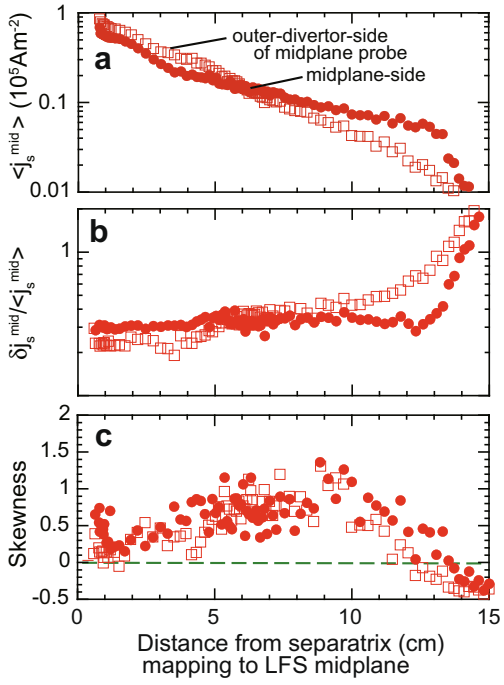

Fig. 5. Radial profiles of (a) $\langle j_s^{mid}\rangle$, (b) $\delta j_s^{mid}/\langle j_s^{mid}\rangle$, (c) *Skewness*, for the midplane (closed squares) and the outer-divertor (open squares) sides of the midplane Mach probe for higher $\bar{n}_e = 2.4\times10^{19}$ m^{-3}.

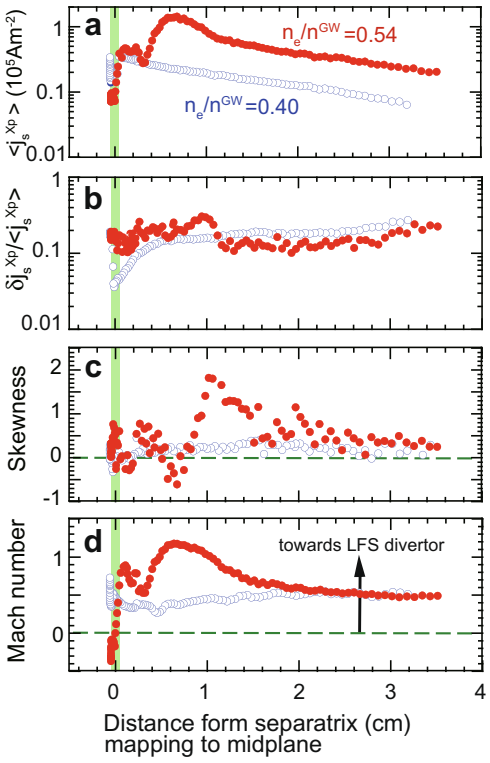

Fig. 6. Comparison of radial profiles: (a) $\langle j_s^{Xp\text{-}m}\rangle$, (b) $\delta j_s^{Xp\text{-}m}/\langle j_s^{Xp\text{-}m}\rangle$, (c) *skewness*, (d) Mach number of the parallel plasma flow, for $\bar{n}_e = 1.7\times10^{19}$ m^{-3} (squares) and 2.4×10^{19} m^{-3} (circles). In the higher $\bar{n}_e$ case, a partial divertor detachment occurs near the separatrix in the outer divertor, and extends to near the X-point ($r^{mid} < 0.5$ cm).

the SOL and divertor plasmas are attached along the field lines. Particularly S^{Xp-m} changes from negative to positive at $r^{mid} \sim 0.8$ cm. This result suggests that intermittent transport is generated near the boundary of the detached and attached plasmas, and that the radial transport of the fast plasma flow is enhanced towards the outer SOL.

Analysis of conditional average shows the time scale of the large 'burst events'. Fig. 7(a) and (b) show conditional averages of $j_s^{mid\text{-}m}$, $j_s^{mid\text{-}d}$ and V_f^{mid} near the separatrix ($r^{mid} = 0.9$ cm) and in the far SOL ($r^{mid} = 5.8$ cm), respectively, for the high density case. The time scale of large 'burst events' is 5–6 μs, which is similar to that in the lower $\bar{n}_e$ plasmas as shown in Fig. 3. On the other hand, near the X-point, Fig. 8 shows that the time scale of large 'burst events', which are observed as large positive S^{Xp} (=1.5 and 1.1 at $r^{mid} = 1$

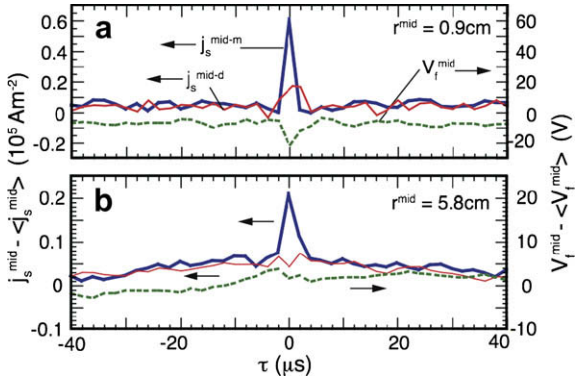

Fig. 7. Conditional averages of $j_s^{mid\text{-}m}$, $j_s^{mid\text{-}d}$ and V_f^{mid} for the high $\bar{n}_e$ case: (a) near the separatrix ($r^{mid} = 0.9$ cm) and (b) in the far SOL ($r^{mid} = 5.8$ cm).

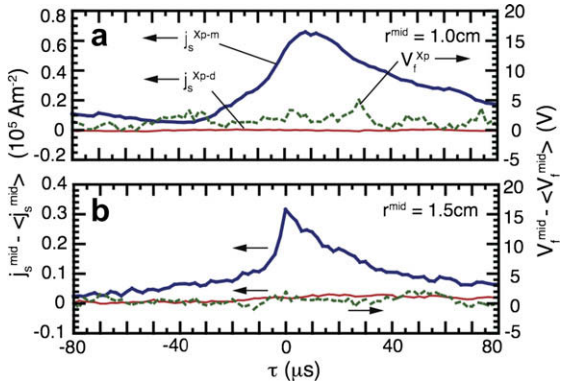

Fig. 8. Conditional averages of $j_s^{Xp\text{-}m}$, $j_s^{Xp\text{-}d}$ and V_f^{Xp} for the high density case: (a) at r^{mid} = 1 cm, (b) at r^{mid} = 1.5 cm, where large positive S^{Xp} (1.8 and 1.1) is observed as in Fig. 6(c).

and 1.5 cm, respectively) in Fig. 6(c), becomes significantly large (40–80 μs). However, correlation with $j_s^{Xp\text{-}d}$ is small, thus the large 'burst events' are transported from the upstream of the Mach probe rather than by radial transport of the filament plasma, and they would enhance the SOL flow towards the divertor.

5. Summary

Understanding of SOL fluctuation characteristics, in particular determination of the intermittent events and their temporal scale, was carried out by applying the statistical analysis of PDF and conditional average to j_s and V_f measured with the Mach probes at the HFS and LFS SOLs in L-mode plasmas. The fluctuation level ($\delta j_s/\langle j_s\rangle$) was found to be large (20–70%) at the LFS midplane, compared to those near the *X*-point (4–20%) and at the HFS SOL (4–10%). Large 'burst events' were observed mostly at the LFS midplane, where positive skewness (S = 0.3–0.8) at the midplane-side of the Mach probe extends over the wide SOL region (r^{mid} < 10 cm), whereas S at the outer-divertor-side becomes large at r^{mid} = 2–6 cm. Time scale of the 'burst events' in j_s was short (~5 μs), and positive correlation between j_s^{mid} at the two sides suggests either the radial or poloidal transport of the filaments.

When the plasma detachment extends to the upstream of the divertor target, i.e. near the X-point, in the high density divertor, large 'burst events' characterized by large positive skewness (up to 1.8) and long time scales of 40–80 μs were observed in the attached SOL area near the *X*-point (0.5 < r^{mid} < 1.5 cm). A small correlation between j_s^{Xp} at the two sides suggests that the large 'burst events' are transported from the upstream main SOL. They can therefore be considered as a candidate mechanism to enhance the radial transport and the SOL flow towards the divertor.

References

[1] J. Terry et al., J. Nucl. Mater. 290–293 (2001) 757.
[2] J.A. Boedo et al., J. Nucl. Mater. 313–316 (2003) 813.
[3] N. Asakura et al., Nucl. Fus. 44 (2004) 503.
[4] N. Asakura, ITPA SOL and divertor topical group, J. Nucl. Mater. 363–365 (2007) 41.